

# MODE I FATIGUE DELAMINATION GROWTH ONSET IN FIBRE REINFORCED COMPOSITES: EXPERIMENTAL AND NUMERICAL ANALYSIS

Man Zhu<sup>1,3</sup>, Larissa Gorbatikh<sup>1,3</sup>, Sander Fonteyn<sup>2,3</sup>, Lincy Pyl<sup>2</sup>, Danny Van Hemelrijck<sup>2</sup>, and Stepan V. Lomov<sup>1,3</sup>

<sup>1</sup> Department of Materials Engineering, KU Leuven, Kasteelpark Arenberg 44 bus 2450, 3001 Leuven, Belgium, [man.zhu@kuleuven.be](mailto:man.zhu@kuleuven.be), [larissa.gorbatikh@kuleuven.be](mailto:larissa.gorbatikh@kuleuven.be), [stepan.lomov@kuleuven.be](mailto:stepan.lomov@kuleuven.be), <http://www.composites-kuleuven.be/>

<sup>2</sup> Department Mechanics of Materials and Constructions, Vrije Universiteit Brussel, Pleinlaan 2, 1050 Brussels, Belgium, [lincy.pyl@vub.be](mailto:lincy.pyl@vub.be), [danny.van.hemelrijck@vub.be](mailto:danny.van.hemelrijck@vub.be), <http://www.vub.ac.be/MEMC/>

<sup>3</sup> SIM M3 program, Technologiepark 935, 9052 Zwijnaarde, Belgium, <http://www.sim-flanders.be/>

**Keywords:** Fatigue delamination growth onset, Mode I, Cohesive zone models, Digital image correlation

## ABSTRACT

Mode I fatigue delamination growth onset in fibre reinforced composite laminates is studied here by experimental and modelling tools. Mode I fatigue growth tests were conducted on Double Cantilever Beam specimens at various load levels. Digital image correlation (DIC) was used to detect movement of the inter-laminar crack tip position during the tests and then to determine the fatigue delamination onset life which is the cycle to onset of delamination growth. The fatigue onset life obtained using the DIC approach is significantly lower than that determined by the compliance monitoring method that is recommended in the ASTM standard. A cohesive zone model was developed to predict the fatigue delamination growth onset in composites. The progressive degradation law developed in the cohesive zone model describes the decrease of the critical strain energy release rate of the interface based on the G-N curve from fatigue delamination growth onset test. The proposed model could successfully reproduce the fatigue delamination onset life of composite laminates.

## 1 INTRODUCTION

Modelling and characterization of fatigue delamination behaviour of fibre reinforced plastics (FRP) are important for understanding and predicting durability and damage tolerance of composite structures. The fatigue delamination growth onset test is commonly used to characterize the inter-laminar fatigue behaviour of FRP composites under cyclic loading. This test measures the number of cycles (N) before an existing delamination crack starts growing under a certain loading level (G), and this is described by a G-N curve [1]. The growth onset test describes the fatigue damage of a material at the crack tip and gives an important reference for the fatigue no-growth design of FRP composite structures.

At present, the G-N curve is commonly obtained by performing a Mode I fatigue growth onset test according to ASTM D6115 standard [2]. Three different ways are introduced in the standard to determine the crack growth onset. These are: (1) visual observation; (2) detection of 1% increase in system's compliance; (3) detection of 5% increase in system's compliance. Because of the difficulties in visual monitoring of the crack tip, compliance-monitoring-based methods are recommended in the standard. As the compliance characterises the full sample deformation resistance rather than precisely the crack growth onset, the compliance-based method is prone to errors [1]. To overcome this difficulty, several methods have been developed in recent years to improve the accuracy of the delamination growth detection in composites, including the electric potential-based method [3], wave-based methods [4] and acoustic emission techniques [5]. However, these studies have been limited to

either quasi-static loading conditions or/and small-size specimens. Few studies focused on the in-situ detection of delamination development under fatigue loads.

Apart from experimental studies, the fatigue delamination of composites has also been studied numerically using finite-element (FE) models. In these modelling works, cohesive zone models (CZMs) have been used due to their success in the simulation of quasi-static delamination. In most CZMs, the damage evolution at the interface during fatigue loading is calculated based on Paris' law obtained from fatigue delamination propagation tests [6-9]. One may question validity of such an approach, as Paris' law is a macroscopic description of the crack growth, while the CZMs rely on local pointwise evaluation of fatigue damage. Consequently, some theoretical assumptions are further required to physically match Paris' law with CZMs, for example, the definition of a cohesive zone [6, 8]. The physical meaning and validity of these assumptions are still an open topic of discussion. Compared to the Paris' law, the test for fatigue delamination growth onset focuses on the delamination behaviour ahead of a crack tip, which directly reflects the local concept of CZMs.

In this work a new method based on DIC is proposed to detect the delamination growth under fatigue loading. The accuracy of the crack tip position obtained from the new method is verified by microscope observations. A CZM based on the measured G-N curve is also developed for modelling the Mode I fatigue delamination growth onset.

## 2 MODE I FATIGUE DELAMINATION GROWTH ONSET EXPERIMENT

To characterize the mode I fatigue delamination growth onset, fatigue tests were performed using DCB specimens. In this section experimental details about the specimens, test procedure and data processing method are presented.

### 2.1 Material and specimen configuration

The composite laminates used in this work have 18 layers of 0° unidirectional PYROFIL™ carbon/epoxy from Mitsubishi Rayon Co., Ltd. A 12.5 µm PTFE film was placed in the middle plane to act as an initial delamination. The specimens were nominally 150 mm long, 25 mm wide and 4.2 mm thick with a 50 mm PTFE insert at one end of the specimen. The speckle patterns were applied at the edge of the specimens for the following DIC processing. Two aluminium load-blocks were adhesively bonded onto the specimen's end for load introduction.

### 2.2 Fatigue delamination growth onset test procedure

In the fatigue tests, specimens were loaded under a constant displacement amplitude process with the ratio of minimum/maximum displacement  $R = 0.1$ . The frequency of the fatigue test was 10 Hz. Images of the fatigue crack extension on one side of the specimen were automatically recorded at a maximum displacement during the fatigue tests with two digital cameras which were synchronized with the testing machine. A photograph of the test set-up is shown in Figure 1.

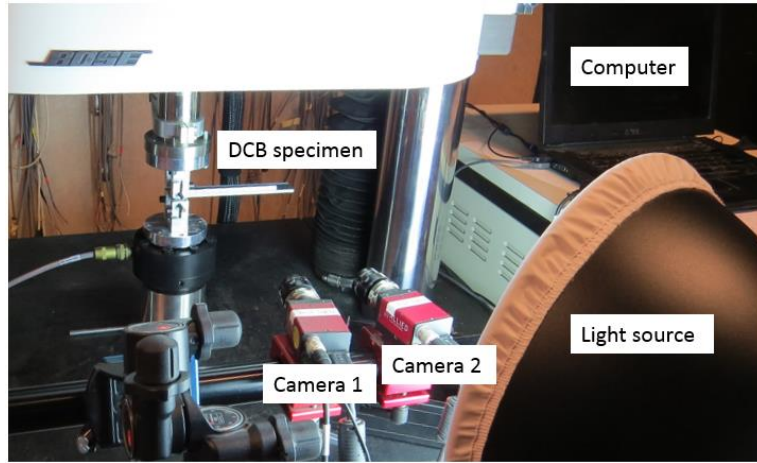


Figure 1: Test set-up.

### 2.3 Crack tip detection with DIC

With a commercial software Vic-3D<sup>TM</sup>, the vertical displacement field,  $V$ , at the edge of the DCB specimens was obtained with the resolution of 1 pixel = 37  $\mu\text{m}$ . An example of the vertical displacement field close to the crack path is shown in Figure 2 for cycle 20 (the displacement of the specimen due to its small rotation was eliminated). The vertical displacement varies along the thickness direction because of the opening of the crack and this variation gradually decreases to zero as the analysis point approaches the crack tip. The crack tip position could be detected through finding a zero variation of the vertical displacement (seen as green zone of displacement field  $V$ ).

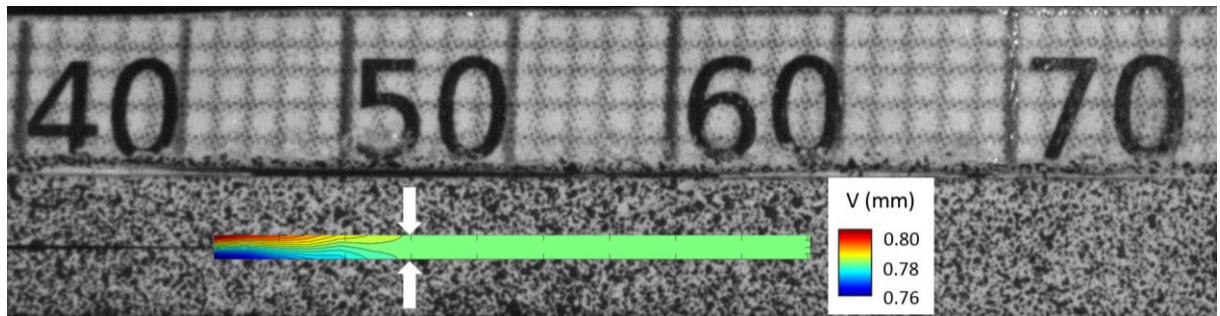


Figure 2: The vertical displacement field  $V$  for cycle 20. Crack tip position is shown with arrows.

### 2.4 Determination of fatigue onset life

The new crack tip detection method was used to determine the progression of the crack tip with cycles (i.e. crack growth curve). Fatigue onset life  $N_{\text{onset}}$  (defined as the cycle number at which the crack starts growing) could be determined by detecting movement of the crack tip position. The crack growth curve expression is described as

$$x = f(N) = \begin{cases} a_0, & N \leq N_{\text{onset}} \\ \alpha(N - N_{\text{onset}}) + a_0, & N > N_{\text{onset}} \end{cases}, \quad (1)$$

$$R^2 = \sum_i [f(N_i) - x_i]^2 \rightarrow \min, \quad (2)$$

where  $a_0$  and  $N_{\text{onset}}$  stand for the initial crack length and fatigue onset life, and  $\alpha$  represents the rate of crack growth.  $N_i$  and  $x_i$  are the number of cycles and crack tip position obtained from DIC detection, respectively. Before the fatigue onset life,  $N_{\text{onset}}$ , is reached, the crack doesn't grow and its tip stays at the initial position  $a_0$ . Therefore a constant function was adopted when  $N \leq N_{\text{onset}}$ . A

simple linear fitting function was used to describe the crack growth when  $N > N_{\text{onset}}$ . The fitting parameters were determined according to the least square method  $R^2$  (Eq.(2)). A representative example of the usage of the fitting is shown in Figure 3, in which a 95% confidence band of the fatigue onset life,  $N_{\text{onset}}$ , is also given to evaluate the error of the  $N_{\text{onset}}$  identification.

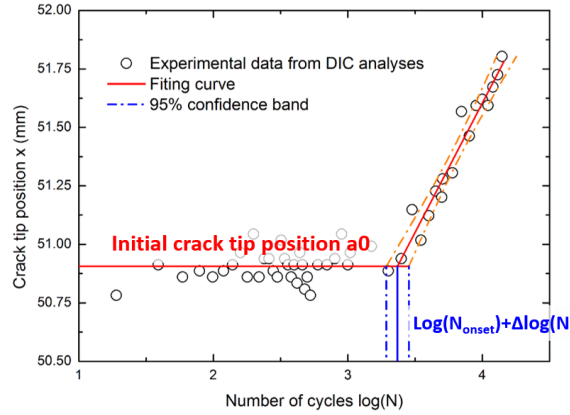


Figure 3: An example of  $N_{\text{onset}}$  identification.

## 2.5 Results and discussion

The proposed crack tip detection method was applied to nine different tests, and the measured initial crack tip position,  $a_0$ , are listed in Table 1. Here both raw data at cycle 20 and fitted data with Eq. (1) are given. To verify the new crack tip detection method, the initial crack lengths obtained from microscope observation are provided for comparison. It indicates that the fitted initial crack length from Eq. (1) exhibits a high accuracy, which differs from microscope observation by less than 0.32 mm. The fitted initial crack tip position and raw data are also of the same magnitude, which implies that the expression Eq. (1) doesn't introduce extra errors.

Specimen number	Microscope observation before the tests (mm)	DIC detection at cycle 20 (mm)		Fitted initial crack length $a_0$ (mm)	
		value	Difference from microscope	value	Difference from microscope
1	52.00	52.02	+0.02	52.07	+0.07
2	51.35	51.13	-0.22	51.21	-0.14
3	50.68	50.83	+0.15	50.93	+0.25
4	48.72	48.42	-0.30	48.40	-0.32
5	48.92	48.67	-0.25	48.69	-0.23
6	52.68	52.71	+0.03	52.80	+0.12
7	49.97	50.17	+0.20	49.97	±0.00
8	49.53	49.79	+0.26	49.26	-0.27
9	49.07	49.41	+0.34	49.10	+0.03

Table 1: Comparison of the initial crack tip positions determined with different techniques.

It is interesting to compare the difference of fatigue onset life obtained by the DIC and conventional compliance monitoring. Figure 4(a) shows a variation of the compliance of the beam arm with a number of cycles for a given specimen. The compliance increase detection yielded a fatigue onset life  $N_{\text{onset}} = 5500$  by detecting 5% increase of compliance. With the use of the mathematical model developed in section 2.4, the present DIC measurement gave  $N_{\text{onset}} = 2600$  cycles. Thus, the fatigue onset life obtained from the DIC method is significantly lower than that from the compliance increase detection method. The same procedure was applied to all specimens, and G-N curves were obtained for the two methods (see Figure 4(b)), respectively. At all loading levels, the DIC method gave shorter fatigue onset life than the conventional compliance increase detection

method. In conclusion, the present DIC method is linked to the real crack opening displacement, and gives more conservative results for fatigue onset life than the compliance monitoring method recommended in ASTM D6115 standard.

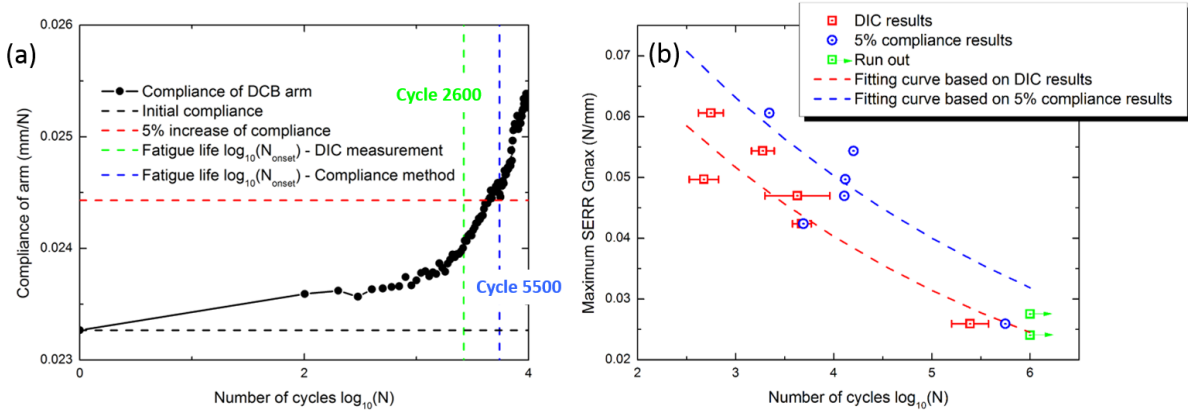


Figure 4: (a) Comparison of fatigue life from DIC measurement and compliance method for one specimen; (b) Comparison of G-N curves from DIC method and compliance method.

### 3 FEM SIMULATION ON MODE I FATIGUE DELAMINATION GROWTH ONSET

This section introduces a new CZM that is capable of modelling the fatigue delamination growth onset in FRP composites. In this model, the progressive damage caused by cyclic loading was simulated as degradation of the critical strain energy release rate (SERR) with cyclic number.

#### 3.1 Cohesive zone model

A bilinear constitutive law was adopted to describe the interfacial behaviour under quasi-static loading as shown in Figure 5(a).  $\delta_0|_{\text{static}}$  and  $\delta_f|_{\text{static}}$  stand for the displacement corresponding to damage initiation and full failure, respectively. The critical SERR,  $G_c|_{\text{static}}$ , is the area under the quasi-static stress-strain curve, which represents the strain energy dissipated during formation of a unit of a new surface. Once the externally applied SERR equals to  $G_c|_{\text{static}}$ , the cohesive element fails completely and a new crack surface is formed.

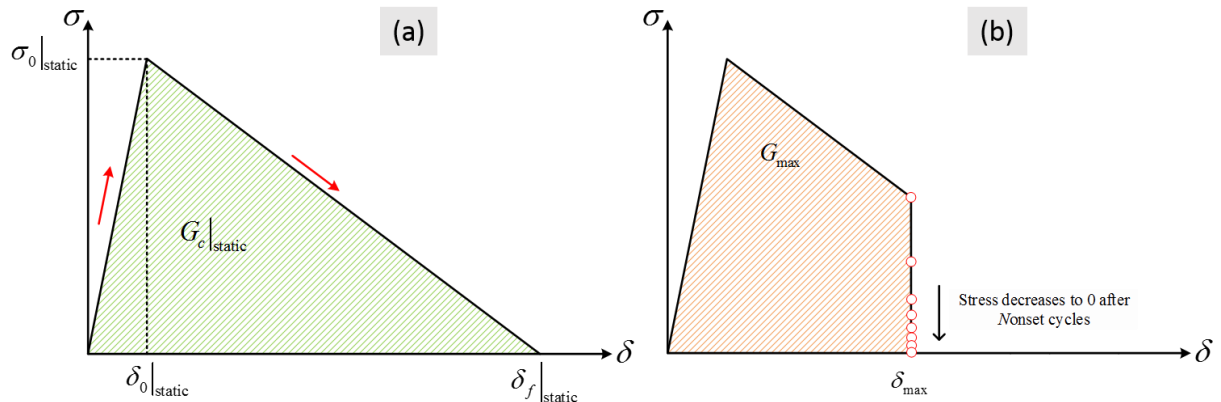


Figure 5: (a) Bilinear constitutive law for static loading; (b) Failure of cohesive element at cycle  $N_{\text{onset}}$ .

As cyclic loading increases damage accumulation ahead of the crack tip relative to the quasi-static case, the crack under fatigue loading starts growing even if the maximum applied SERR,  $G_{\text{max}}$ , is lower than  $G_c|_{\text{static}}$ , that is,  $G_c = G_{\text{max}} < G_c|_{\text{static}}$ . Generally, fatigue onset life ( $N_{\text{onset}}$ ) increases as  $G_{\text{max}}$

decreases, which is described by the G-N curve. Therefore, the degradation law of  $G_c$  can be obtained from the G-N curve, as:

$$\frac{dG_c}{d\ln N} = \frac{G_c|_{\text{static}} - G_{\max}}{\ln N_{\text{onset}}} \Rightarrow \frac{dG_c}{dN} = \frac{G_c|_{\text{static}} - G_{\max}}{N \ln N_{\text{onset}}}, \quad (3)$$

where  $(N_{\text{onset}}, G_{\max})$  corresponds to a point on the G-N curve. The degradation of  $G_c$  can be described as a decrease of the area under the constitutive cohesive law curve. Figure 5(b) shows that the total area under the stress-displacement curve decreases to the applied SERR  $G_{\max}$  when the element has failed after  $N_{\text{onset}}$  cycles.

### 3.2 Simulation of Mode-I delamination

The developed CZM was implemented as a user-written finite element material program in FE software. The FE model of DCB is shown in Figure 7. The arms are composed of 8-node solid elements, which are connected by 8-node cohesive elements. Only one element was built along the width direction and a generalised plane strain boundary condition was applied to the FE model. The quasi-static tests were conducted to get the elastic properties of the used carbon/epoxy UD laminates and the interlaminar properties of  $0^\circ/0^\circ$  interface, which are shown in Table 2. The G-N curve in Figure 4(b) obtained from the new DIC-based method was used as input of the material properties as Equation (4)

$$G_{\max} = CN^n, \quad (4)$$

where C and n are fitting parameters.

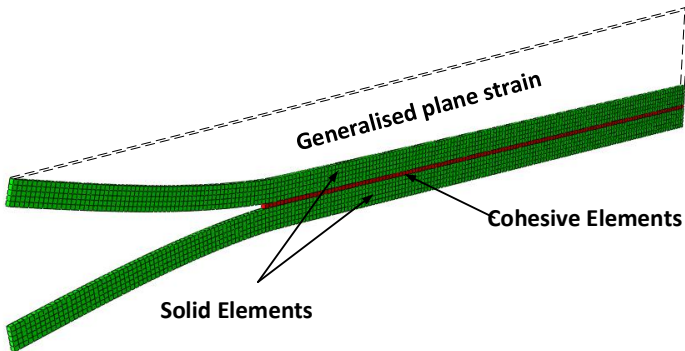


Figure 7: Finite element model of the DCB specimen

Elastic properties	$E_{11}$ [GPa]	$E_{22}=E_{33}$ [GPa]	$\nu_{12}=\nu_{13}$ [-]	$\nu_{23}$ [-]	$G_{12}=G_{13}$ [GPa]	$G_{23}$ [GPa]
	136	9.4	0.33	0.33	4.11	3.53
Interlaminar cohesive properties	$G_c _{\text{static}}$ [N/mm]	$\sigma_0 _{\text{static}}$ [MPa]	$C$ [N/mm]	$n$ [-]		
	0.104	71	0.107	-0.109		

Table 2: Material properties for UD laminates

The simulation was performed under the Mode I condition. The DCB model was firstly loaded to the maximum displacement statically, and the cohesive elements follow the static bilinear constitutive law in this stage. After the maximum displacement was reached, the fatigue damage law was triggered. The maximum load in cycles is maintained, and the pseudo-time increment in FE analysis

was assumed to be proportional to the number of loading cycles. On this basis, the fatigue damage accumulation was taken into account in the CZM. The fatigue delamination growth onset was determined by complete failure of the cohesive element ahead of the crack tip. In Figure 8, the simulated fatigue onset life under different loading levels are compared with the measured G-N curve, which indicates a good agreement between simulation and experimental results.

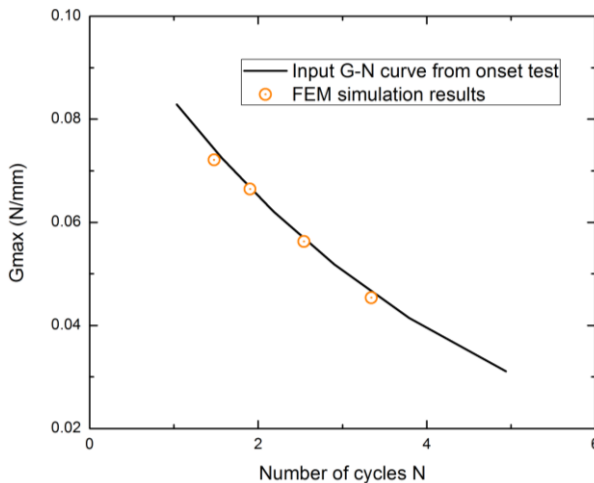


Figure 8: FEM simulation results of Mode I fatigue growth onset based on the experimental G-N curve

#### 4 CONCLUSIONS

A DIC-based crack tip detection method is proposed to determine Mode I fatigue onset life of composite laminates. The fatigue onset life obtained from the DIC measurement is significantly lower than that based on 5% of the compliance increase. A CZM was developed based on a G-N curve from the experimental growth onset test. The model successfully reproduces the input experimental data by modelling the crack growth onset as the failure of the cohesive element at the crack tip, and the next step of the work is to validate the model on independent test cases.

#### ACKNOWLEDGEMENTS

The work has been funded by the SBO project “M3Strength”, which fits in the MacroModelMat (M3) research program funded by SIM (Strategic Initiative Materials in Flanders) and VLAIO (Flanders Innovation & Entrepreneurship).

#### REFERENCES

- [1] B.L.V. Bak, C. Sarrado, A. Turon and J. Costa, Delamination under fatigue loads in composite laminates: a review on the observed phenomenology and computational methods, *Applied Mechanics Reviews*, **66**, 2014, pp. 060803.
- [2] ASTM D6115-97, Standard test method for mode I fatigue delamination growth onset of unidirectional fibre reinforced polymer matrix composites, ASTM International, 2011
- [3] M. Zappalorto, F. Panizzo, P.A. Carraro and M. Quaresimin, Electrical response of a laminate with a delamination: modelling and experiments, *Composites Science and Technology*, **143**, 2017, pp. 31-45.
- [4] D. Wang, L. Ye, Y. Tang and Y. Lu, Monitoring of delamination onset and growth during Mode I and Mode II interlaminar fracture tests using guided waves, *Composites Science and Technology*, **72**, 2012, pp. 145-151.
- [5] M. Saeedifar, M. Fotouhi, M.A. Najafabadi, H.H. Toudehsky and G. Minak, Prediction of quasi-static delamination onset and growth in laminated composites by acoustic emission, *Composites Part B: Engineering*, **85**, 2016, pp. 113-122.

- [6] A. Turon, J. Costa, P. Camanho and C. Davila, Simulation of delamination in composites under high-cycle fatigue, *Composites Part A: Applied Science and Manufacturing*, **38**, 2007, pp. 2270-2282.
- [7] B.L. Bak, A. Turon, E. Lindgaard and E. Lund, A simulation method for high-cycle fatigue-driven delamination using a cohesive zone model, *International Journal for Numerical Methods in Engineering*, **106**, 2016, pp. 163-191.
- [8] P.W. Harper and S.R. Hallett, A fatigue degradation law for cohesive interface elements—development and application to composite materials, *International Journal of Fatigue*, **32**, 2010, pp. 1174-1787.
- [9] L.F. Kawashita and S.R. Hallett, A crack tip tracking algorithm for cohesive interface element analysis of fatigue delamination propagation in composite materials, *International Journal of Solids and Structures*, **49**, 2012, pp. 2898-2913.